SYNCELL

WHITE PAPER

# Unveiling Primary Ciliary Proteins with Microscoop™

June. 2024 | #WP002


**Authors**

Hsiao-Jen Chang, Chantal Hoi Yin Cheung, and Hsuan-Hsuan Lu

# Introduction

Primary cilia are microtubule-based organelles extending from the surface of most mammalian cells, playing pivotal roles in signal transduction and cellular functions[1]. Malfunctions of primary cilia are implicated in a number of genetic disorders termed ciliopathies, including polycystic kidney disease[2], Bardet-Biedl syndrome[3], and Joubert syndrome[4]. These conditions adversely affect organs such as the kidneys, retina, and brain, influencing key biological processes like cell cycle regulation and tissue development. The study of primary cilia, despite their significance, is filled with challenges. The organelles' diminutive size and structural delicacy significantly complicate their analysis. Additionally, the dynamic nature of their assembly further complicates their study, necessitating high-resolution techniques for detailed analysis.

Addressing these challenges, the Microscoop™ platform emerges as an advancement in biological research technology, particularly enhancing the capability for spatial photolabeling at the microscale. It enables the in-depth investigation of primary cilia, providing the necessary precision and detail to comprehensively explore their biological function. With the potential to transform our understanding of ciliary functions in both health and disease, its application in proteomic analysis demonstrates its utility in unraveling the complex protein constitutes of primary cilia, essential for elucidating cellular mechanisms and pathogenesis.

# Capturing and analyzing primary cilia with Microscoop™

The Microscoop™ platform is designed for the isolation and identification of proteins within submicron cellular regions, specifically aiming to target and analyze subcellular organelles such as primary cilia. It combines a motorized epifluorescence microscope, a high-resolution sCMOS camera, and a two-photon light source. This system is further enhanced by a specially developed photochemical probe (Fig. 1), allowing for precise targeting and isolation of primary cilia for proteomic analysis. To facilitate visualization, primary cilia are pre-stained with the well-known marker polyglutamylation modification (GT335). Real-time image analysis is employed to segment the primary cilia and filter out non-specific signals, using a combination of thresholding, size and length exclusion, and morphological recognition techniques. This ensures efficient segmentation of each Field of View (FOV) image for identifying primary cilia, thereby enabling effective path planning and labeling control. Through the use of two-photon illumination, the system triggers photochemical agents to photo-biotinylate proteins within the primary cilia. The Microscoop™ platform controls the sequential photo-biotinylation of individual primary cilia via mechatronic position control, processing millions of primary cilia to collect sufficient proteins for downstream proteomic analysis. The photo-biotinylated proteins are then subjected to streptavidin pull-down, followed by hypothesis-free mass spectrometry (LC-MS/MS) analysis, facilitating a comprehensive proteomics discovery. By integrating ultrahigh-content, high-speed microscopy with targeted photo-biotinylation, the Microscoop™ platform revolutionizes the study of primary cilia, enabling spatial isolation for proteomic discovery.

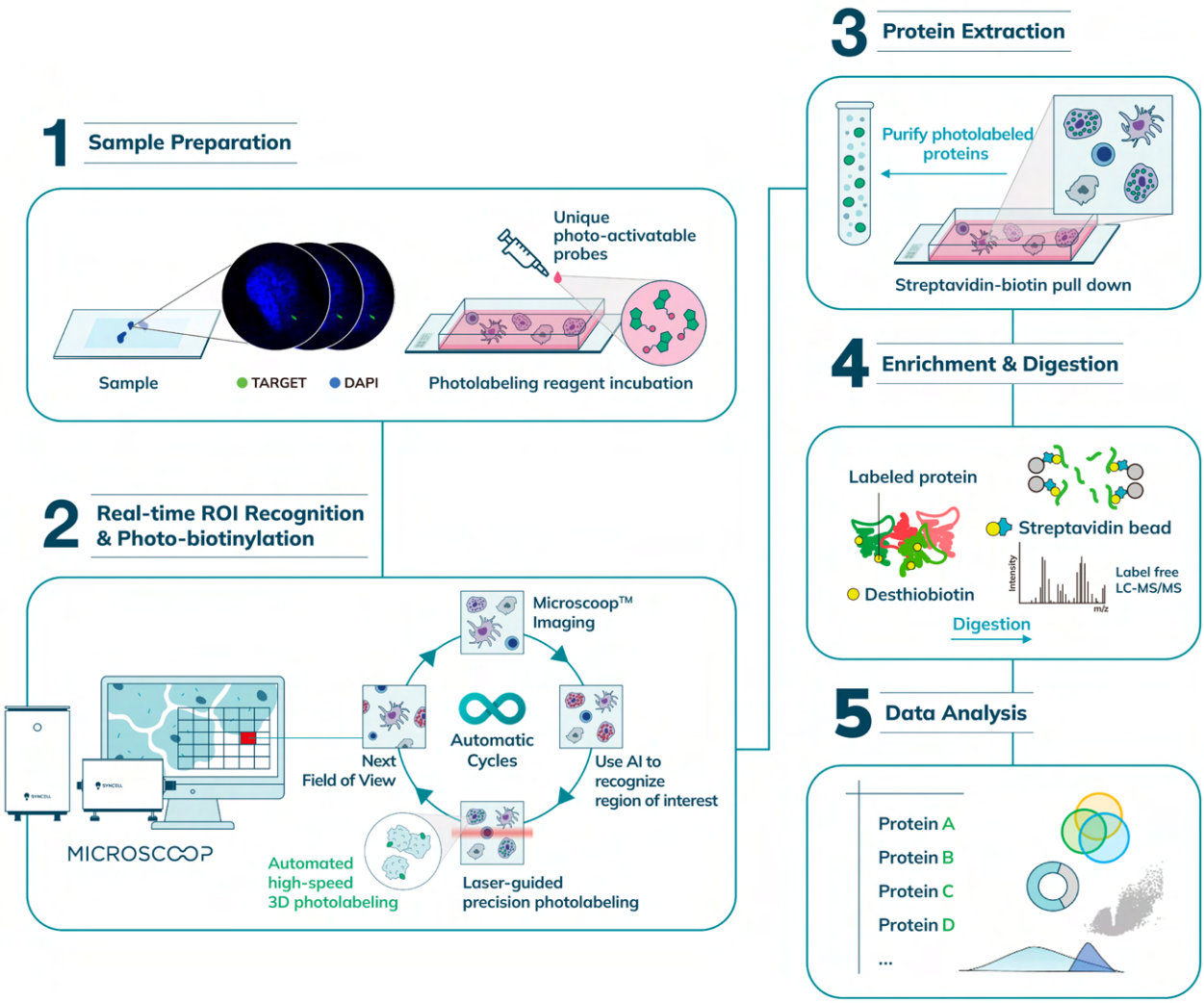


Fig. 1 | Schematic workflow for mapping the primary cilia proteome. A microscopy-guided protein discovery platform integrates image acquisition, photochemistry, microscopy, optics, and mechatronics enables ultrahigh-content *in situ* photolabeling followed by mass spectrometry analysis.

Microscoop™ has been engineered to enable photolabeling at the subcellular level, targeting ROIs such as primary cilia, which are presumed to have uniform protein constituents identifiable by distinct morphological features and contrast under microscopy. This method involves several steps executed millions of times: 1) employing microscopy to identify primary cilia; 2) capturing images; 3) processing images to eliminate background noise; 4) recognizing primary cilia patterns; 5) illuminating within primary cilia for photochemical labeling; 6) transitioning to the next FOV (Fig. 2). This repetitive process is crucial for spatially isolating proteins, thereby gathering enough proteins to address the challenge of protein amplification. Remarkably, existing technologies lack the capability for such extensive and rapid repetition across locations and timespans.

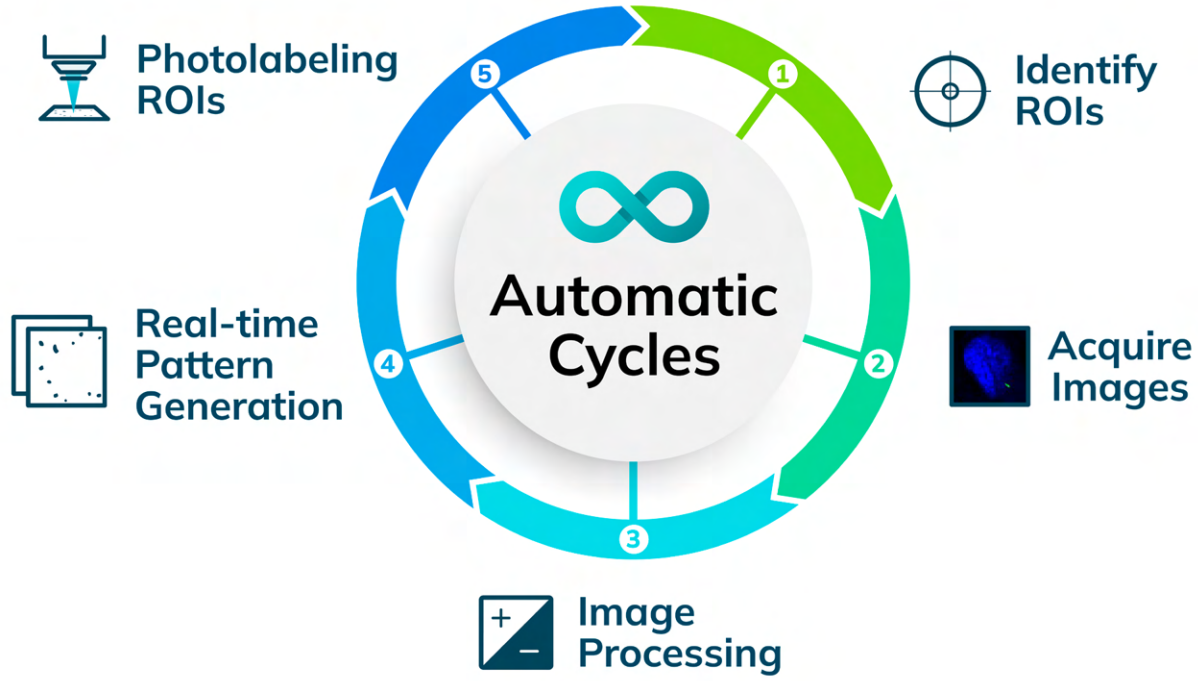


Fig. 2 | The process and design of the microscopy-guided protein isolation platform. The process includes: (1) identifying the primary cilia by light microscopy; (2) acquiring images of primary cilia; (3) processing images to identify primary cilia as ROIs; (4) generating realtime patterns of ROIs; (5) illuminating the selected region within ROIs for protein photo-biotinylation; (6) moving the stage to the next FOV; and repeating steps 1-5 for each FOV until all FOVs of intereest have been processed.

The images are processed in real-time to segment the primary cilia using image processing techniques, including thresholding, filtering, size and length exclusion, and morphological recognition. These steps are uniformly applied across all FOVs, with pre-processing or post-processing adjustments to ensure consistent image quality. The segmentation results, depicted in Figure 3, require 0.1 to 1 second for completion, varying with the image's complexity and quality. Following segmentation, the coordinates of the primary cilia's grid points are determined. A planned path for photochemical activation is then optimized and used to guide the galvanometers (galvos) across these points. The galvos and the Acousto-Optic Modulator (AOM) synchronize to within approximately 100 microseconds, enabling precise control over the locations and duration, thus ensuring a consistent photochemical reaction across all spots. For locations with multiple primary cilia, the scanning path sequentially targets each cilium, initiating at the periphery and spiraling clockwise towards the center before proceeding to the next cilium's starting point. This method reduces travel time and minimizes mechanical stress on the galvos. Achieving this level of intricacy within a feasible timeframe relies on speed optimization, seamless automation, and accurate mechatronic control throughout the process.

To validate the labeling accuracy and precision for primary cilia as small as 0.2 μm in width and 1 μm in length, primary cilia of RPE-1 cells were pre-stained with GT335, followed by photo-biotinylation using Microscoop™. The platform accurately recognized primary cilia, enabling targeted spatial photolabeling with two-photon illumination. This method facilitated the isolation of primary cilia proteins with high specificity, as demonstrated by the congruence between the *in situ* biotinylated regions (green) and the primary cilia (red) fluorescence in both lateral (xy) and axial (z) directions (Fig. 3, right panel).

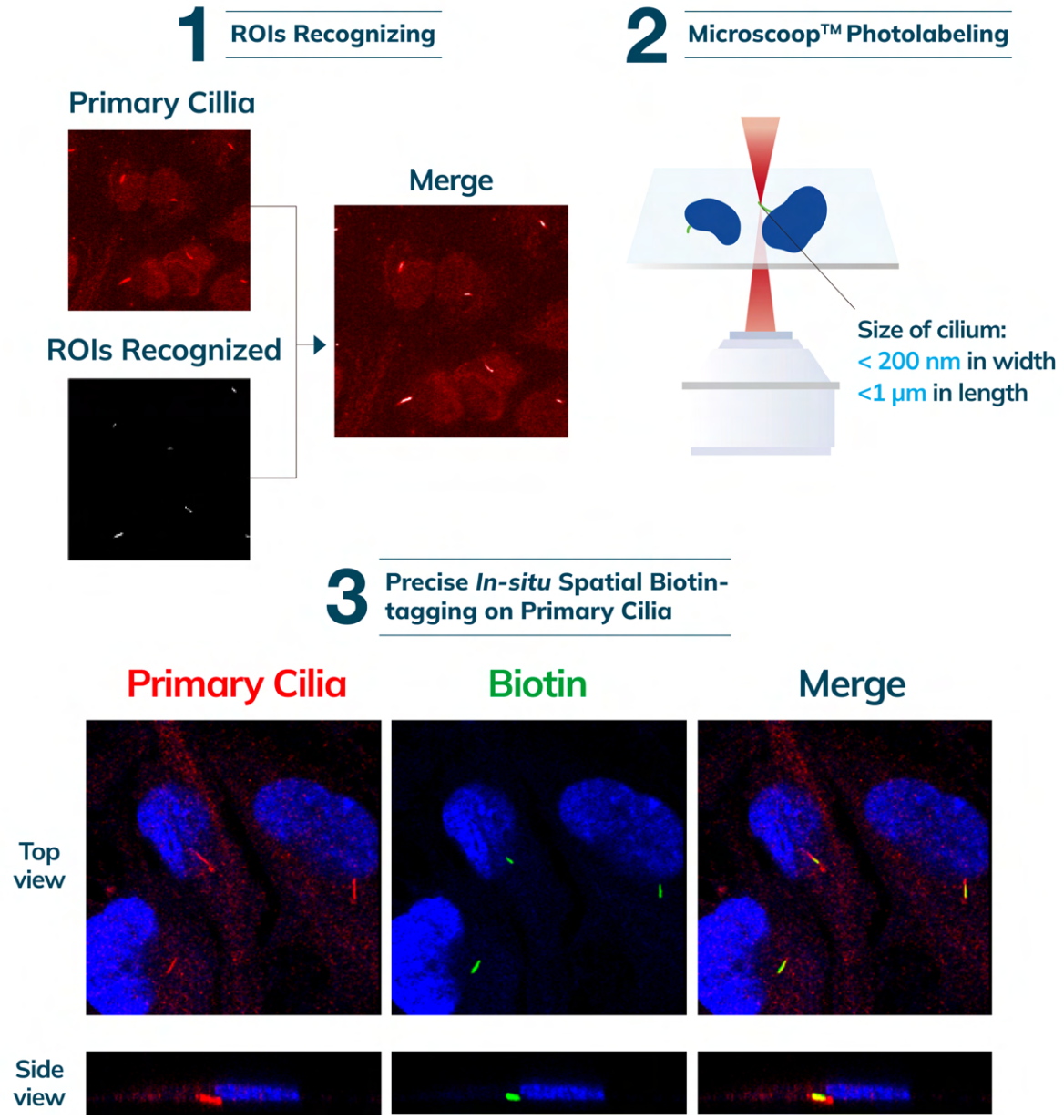


Fig. 3| Primary cilia are processed by filtering and segmentation by image processing (left), Confocal micrographs depicting precise and accurate photolabeled primary cilia at lateral (xy)- and axial (z) directions (right). Red: GT335, Green: NeutrAvidin-488, Blue: DAPI.

## Unveiling ciliary proteins andfunctional insights

Photolabeling experiments were conducted on PFA fixed RPE-1 cells, specifically targeting regions marked with GT335 to elucidate the protein composition of primary cilia (Fig. 4A). Following hours of precise photolabeling, cells were harvested and lysed to extract proteins. The photolabeled proteins were subsequently enriched through streptavidin bead pulldown, digested with trypsin, and analyzed via LC-MS/MS. This comprehensive analysis resulted in the high-confidence identification of 4,233 proteins (Figure 4B) and a total of 608 ciliary proteins were identified among experiments (Figure 4C). Among the identified proteins, key ciliary trafficking components such as intraflagellar transport proteins (IFTs), kinesins, dyneins, GTPases, and phosphatidylinositol phosphates (PIPs) were enriched, exhibiting high photolabeling to control (PL/CTL) ratios (Fig. 4D). Additionally,

proteins involved in structural support and cellular organization, including microtubules, septins, and annexins, were also observed to be enriched within the photolabeled sample.

Gene ontology (GO) enrichment analysis further validated these findings, demonstrating a significant association of the enriched proteins with critical biological processes such as ciliary assembly, transportation, and signaling, underpinning the complex functionality of the ciliary proteome (Fig. 4E). Notably, proteins involved in intraciliary transport, a crucial aspect of cilium assembly, were significantly overrepresented in the GO category related to this process. These findings support the effectiveness of targeted photolabeling and proteomic analysis in revealing the network of proteins essential for ciliary function and structure.

Furthermore, 427 ciliary proteins showing significant enrichment in the photolabeled group, indicative of their specific association with primary cilia. These 427 known ciliary proteins were subjected to Reactome pathway analysis, revealing major ciliary pathways such as intraflagellar transport, cilium assembly, signal transduction, cellular responses to stimuli and stress, cell cycle regulation, autophagy, and organelle biogenesis and maintenance (Fig. 4F). Intraflagellar transport and cilium assembly are essential for the movement of molecular cargo along the cilia, ensuring proper ciliary assembly and function. Signal transduction pathways are critical for cilia in transmitting extracellular signals to the interior, influencing various cellular responses. The involvement of ciliary proteins in the cell cycle highlights the importance of cilia in regulating cell division and growth. Autophagy and organelle biogenesis and maintenance pathways underscore the role of cilia in cellular housekeeping and the recycling of cellular components. These pathways are crucial for ciliary function and development, covering a significant portion of the identified ciliary proteome.

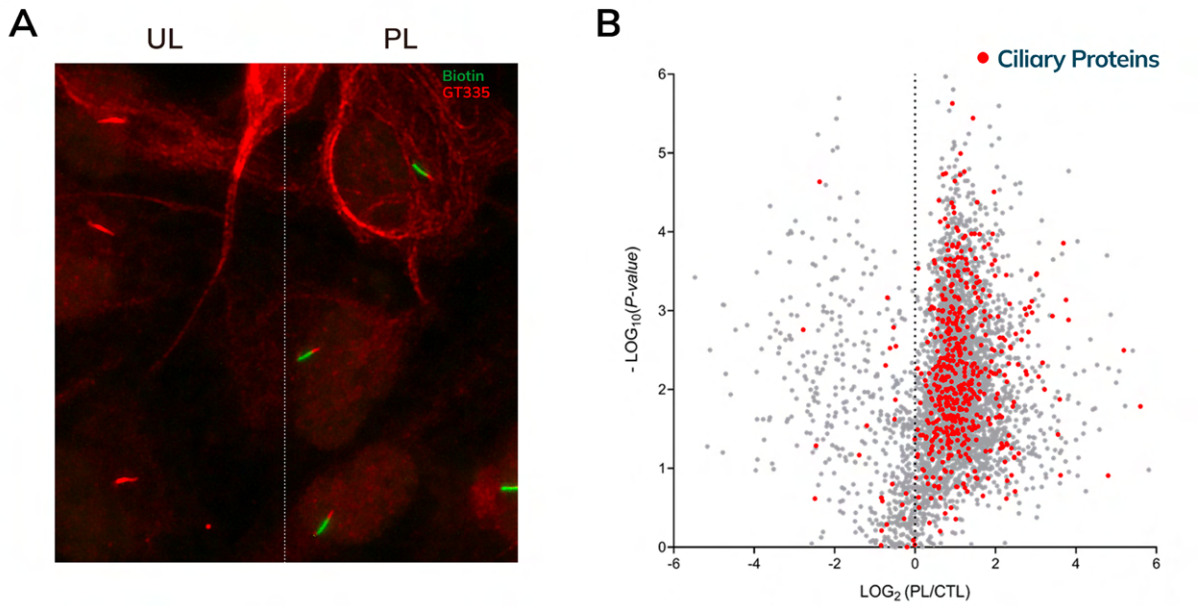

C

## Photo-biotinylation Enriched Primary Cilia Proteins

| | | | | | | | | | | | |
|---|---|---|---|---|---|---|---|---|---|---|---|
| ABCC4 | ATG3 | CEP112 | CTTN | ELMO2 | HSPA4L | KIF23 | MYO1E | PCM1 | QKI | SDCCAG8 | TNS3 | WDHD1 |
| ABLIM1 | ATG5 | CEP120 | CUL3 | ELP4 | HSPA5 | KIF24 | MYO1F | PCNT | RAB10 | SEC23A | TOGARAM2 | WDR1 |
| ABRAXAS2 | ATG7 | CEP128 | CYFIP2 | EML1 | HSPA8 | KIF2A | MYO3B | PDCD6IP | RAB11A | SEC63 | TP53BP1 | WDR11 |
| ACLY | ATP1A1 | CEP131 | CYLD | EPB41L3 | HSPBP1 | KIF2C | MYO5A | PDE1C | RAB13 | SEPTIN10 | TPM3 | WDR12 |
| ACOT9 | ATP1B1 | CEP135 | CYP51A1 | EPS15 | HSPD1 | KIF3A | MYO5C | PDGFRA | RAB14 | SEPTIN11 | TRABD | WDR13 |
| ACTN1 | ATP2A2 | CEP152 | DCTN1 | EPS8L2 | HUWE1 | KIF3B | MYO6 | PDIA6 | RAB18 | SEPTIN2 | TRAPPC10 | WDR18 |
| ACTN4 | ATP2B4 | CEP164 | DCTN2 | ERC1 | HYDIN | KIF4A | MYO9A | PDXDC1 | RAB1B | SEPTIN6 | TRAPPC3 | WDR19 |
| ACTR1A | ATP6V0D1 | CEP170 | DCTN3 | EXOC3 | HYOU1 | KIF5B | MYO9B | PEX6 | RAB21 | SEPTIN7 | TRAPPC9 | WDR24 |
| ACTR2 | ATP6V1A | CEP170B | DCTN4 | EXOC4 | IDE | KIF5C | MYOF | PFKM | RAB23 | SEPTIN8 | TRIM32 | WDR26 |
| ACTR3 | ATP6V1D | CEP192 | DDX1 | EXOC5 | IFIT3 | KIF7 | NAXE | PFN2 | RAB2A | SEPTIN9 | TRIM59 | WDR3 |
| ADCY3 | ATXN10 | CEP250 | DDX21 | EXOC6 | IFT122 | KIFAP3 | NBEA | PIBF1 | RAB32 | SETX | TRIP11 | WDR33 |
| ADD3 | ATXN2L | CEP290 | DDX56 | EXOC6B | IFT140 | KIFBP | NCAPD2 | PIGS | RAB34 | SF3A1 | TSC2 | WDR35 |
| AK1 | AURKA | CEP350 | DDX6 | EZR | IFT172 | KIFC1 | NCAPG | PIK3C3 | RAB35 | SF3B2 | TSG101 | WDR36 |
| AK2 | AXL | CEP43 | DHX30 | FHL2 | IFT27 | KIFC3 | NDC80 | PIK3R4 | RAB3B | SH3GL1 | TTC21B | WDR37 |
| AKAP9 | BBS1 | CEP44 | DHX9 | FKBP5 | IFT52 | KIRREL1 | NDE1 | PIN1 | RAB3C | SHROOM3 | TTF2 | WDR4 |
| AKT1 | BBS2 | CEP57 | DLD | FKBP8 | IFT56 | LAMA5 | NEDD1 | PJA2 | RAB5A | SKP1 | TTLL12 | WDR43 |
| ALMS1 | BBS4 | CEP63 | DLG5 | FLNA | IFT57 | LDHB | NEDD4L | PKD2 | RAB5B | SLAIN2 | TUBA1B | WDR45 |
| ANKMY2 | BBS7 | CEP76 | DMD | FNBP1L | IFT70A | LGALS3 | NEK1 | PKM | RAB5C | SLIRP | TUBA4A | WDR46 |
| ANKS3 | BBS9 | CEP78 | DNAAF5 | FOCAD | IFT74 | LRBA | NEK6 | PLK1 | RAB6A | SLK | TUBA4B | WDR47 |
| ANXA1 | BRI3BP | CEP83 | DNAH11 | GAK | IFT80 | MACF1 | NEK9 | POLA2 | RAB7A | SMARCA4 | TUBB | WDR48 |
| ANXA11 | BSG | CEP89 | DNAJA1 | GANAB | IFT81 | MAP1A | NHERF1 | POLD1 | RAB8A | SMPD4 | TUBB2A | WDR5 |
| ANXA6 | C2CD3 | CEP97 | DNAJB1 | GDI2 | IFT88 | MAP1B | NID2 | POR | RAB8B | SORD | TUBB3 | WDR55 |
| ANXA7 | CALR | CFAP20 | DNM2 | GLE1 | IMPDH2 | MAP1S | NIN | PPA1 | RABEP2 | SPTAN1 | TUBB4A | WDR6 |
| AP2A1 | CALU | CHD4 | DNMT1 | GLOD4 | INPP4A | MAP4 | NME7 | PPIA | RABL3 | SQSTM1 | TUBB4B | WDR62 |
| AP3M2 | CAMK2D | CHORDC1 | DPYSL2 | GLRX3 | INPP4B | MAP4K3 | NOL6 | PPID | RABL6 | SRI | TUBB6 | WDR7 |
| APEX1 | CAMSAP1 | CIT | DROSHA | GMDS | INPP5F | MAP9 | NOTCH2 | PPP1CC | RAC1 | SRR | TUBGCP2 | WDR70 |
| APP | CAMSAP2 | CKAP2 | DSG2 | GNA11 | INPPL1 | MAPKAP1 | NPHP3 | PPP2R1A | RAN | SSX2IP | TUBGCP3 | WDR75 |
| APPL1 | CAPN1 | CKAP5 | DSTN | GOT2 | INTS1 | MAPKBP1 | NPHP4 | PRDX4 | RANBP1 | STAT3 | TUBGCP4 | WDR77 |
| ARF4 | CAPN2 | CLASP1 | DYNC1H1 | GPI | INTS2 | MAPRE1 | NR3C1 | PRIM1 | RANGAP1 | STIP1 | TUBGCP6 | WDR81 |
| ARFGEF2 | CAPZB | CLIC1 | DYNC1I2 | GRK2 | IPO5 | MDC1 | NUDC | PRKAA1 | RAPGEF2 | STK33 | TXNIP | WDR82 |
| ARHGAP1 | CARS1 | CLTB | DYNC2H1 | GSK3B | IQCE | MDM1 | NUP210 | PRKAR1A | RBM22 | SUPT5H | TXNL1 | WDR90 |
| ARHGAP29 | CASK | CLTC | DYNC2I1 | GSN | ITGA3 | MED16 | NUP214 | PRKAR2A | RHOT1 | SURF4 | UBA1 | WDR91 |
| ARHGAP35 | CAV1 | CLUAP1 | EEF1A1 | HAT1 | JPT2 | MICAL3 | NUP35 | PRKAR2B | RICTOR | SYNE1 | UBA6 | WIZ |
| ARHGEF18 | CBL | CNOT10 | EFCAB7 | HAUS1 | KATNAL1 | MLEC | NUP37 | PRKCA | RO60 | SYNE2 | UBAP2L | WRAP73 |
| ARL13B | CC2D2A | CNTRL | EFHC1 | HAUS3 | KATNAL2 | MPDU1 | NUP62 | PRKD2 | RPA1 | TAGLN2 | UBE3C | YTHDF3 |
| ARL14EP | CCDC191 | COL18A1 | EFTUD2 | HAUS4 | KATNB1 | MROH2B | NUP93 | PSMB4 | RPGRIP1L | TAPT1 | UBE4B | YWHAE |
| ARL2 | CCDC61 | COPG1 | EGFR | HAUS5 | KDM3B | MSN | OCRL | PSMC2 | RPL9 | TARS1 | UGGT1 | YWHAG |
| ARL3 | CCDC88A | COPG2 | EHD1 | HAUS6 | KHSRP | MTCL1 | ODF2 | PSMC3 | RPS6KA1 | TBC1D31 | USP9X | YWHAQ |
| ARL6 | CCP110 | COPS8 | EHD3 | HDAC1 | KIF11 | MXRA8 | OFD1 | PSMC5 | RPTOR | TCHP | VCAN | ZC2HC1A |
| ARL6IP4 | CCT2 | CORO1B | EIF2A | HHIP | KIF13A | MYADM | OGFR | PSMD14 | RRM1 | TCP1 | VCL | ZFYVE19 |
| ARL6IP5 | CCT3 | CROCC | EIF2S1 | HK1 | KIF13B | MYCBP2 | ORC1 | PSMD5 | RTCA | THBS1 | VCP | ZFYVE26 |
| ARL6IP6 | CCT4 | CSNK1A1 | EIF3A | HMGB2 | KIF14 | MYH10 | OSBPL6 | PTBP1 | RTN4 | THOP1 | VDAC2 | ZNF318 |
| ARL8B | CCT5 | CSNK2B | EIF4B | HNRNPLL | KIF16B | MYO10 | P4HA1 | PTK2 | RUVBL1 | TIGAR | VDAC3 | ZSCAN18 |
| ARMC9 | CCT8 | CSRP1 | EIF4H | HSP90AA1 | KIF1B | MYO18A | PACS1 | PTPN23 | RUVBL2 | TJP2 | VPS13A | ZWILCH |
| ASAP1 | CDK1 | CSTB | EIF5A | HSP90AB1 | KIF1C | MYO19 | PAFAH1B1 | PTPRK | SCCPDH | TMEM231 | VPS35 | |
| ASNS | CDK5RAP2 | CTNNA1 | EIF6 | HSP90B1 | KIF20A | MYO1B | PAPSS1 | PUM1 | SCD | TMPO | VTN | |
| ATG16L1 | CENPF | CTNNB1 | EIPR1 | HSPA4 | KIF22 | MYO1C | PARD3 | PXDN | SCD5 | TNPO1 | VWA5A | |

Well-known Ciliary Proteins

D

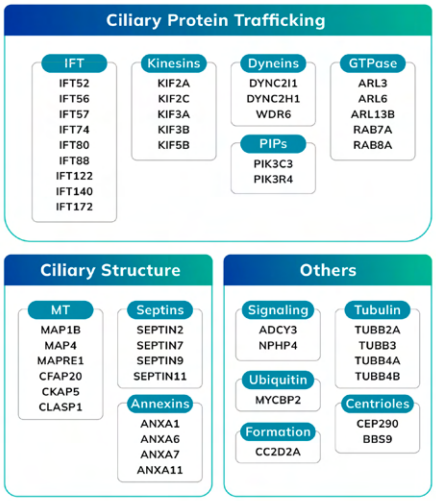


E

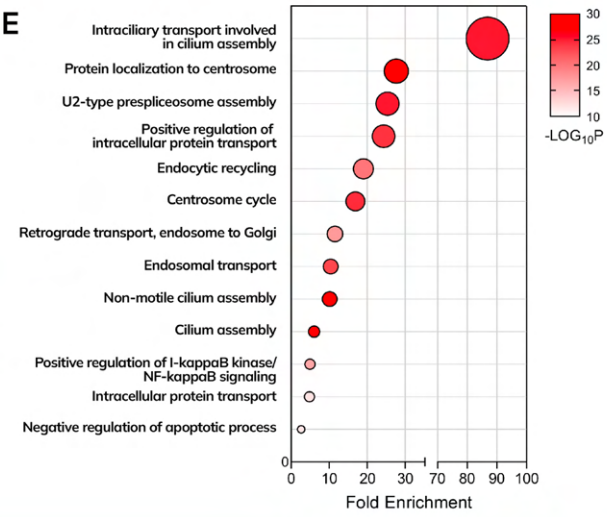


F

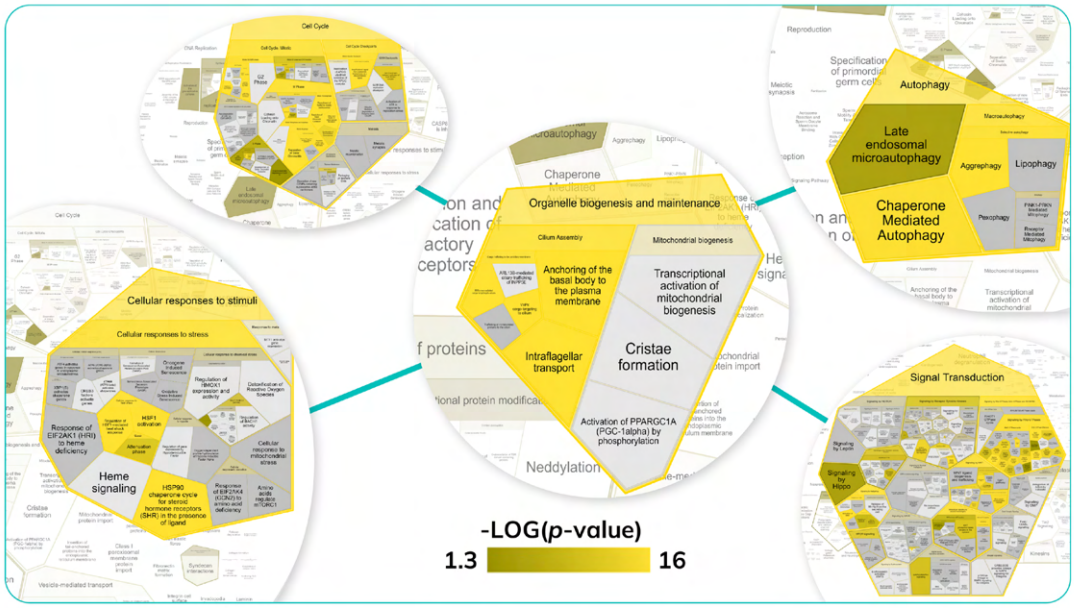

Fig. 4 | (A) Confocal micrographs of unphotolabeled (UL) and photolabeled (PL) at user defined primary cilia. (B) A distribution of overall protein abundances is binned by the ratio of copies in a photolabeled (PL) sample to those in a control (CTL) sample annotated as PL/CTL ratio. Ciliary proteins (red) are enriched in the PL group compared to the CTL sample. (C) 608 ciliary proteins identified by Microscoop™. (D) Well-known cilia proteins identified by Microscoop™. (E) The top 100 enriched proteins were subjected to Gene ontology to reveal cilia related biological process. (F)427 enriched ciliary proteins were subjected to Reactome to reveal cilia related pathways.

# Discovery of novel ciliary proteins

To further explore potential ciliary proteins, we analyzed the top 30 most abundant non-ciliary proteins, referred to as putative ciliary proteins (Fig. 5A). Biological process analysis revealed that these putative ciliary proteins are highly associated with cellular protein localization, protein transport, and regulation of protein stability. These functions are closely related to ciliary activities, suggesting that these proteins may have important roles in ciliary biology (Fig. 5B). Protein-protein interaction network analysis demonstrated that many of these putative ciliary proteins (red circles) interact with the 427 identified ciliary proteins, indicating their potential involvement in ciliary functions (Fig. 5C). These interactions suggest that putative ciliary proteins might participate in crucial processes such as protein trafficking to the cilium, stabilization of ciliary structures, and modulation of ciliary signaling pathways. These findings highlight the significance of these proteins in maintaining the structural and functional integrity of cilia. Moreover, the network analysis revealed specific clusters of interactions where putative ciliary proteins are closely connected with well-known ciliary proteins (black circles). This clustering suggests a coordinated role in ciliary maintenance and function, potentially uncovering new regulatory mechanisms within the cilium. These insights provide a deeper understanding of the protein network dynamics within cilia and highlight the complexity of ciliary protein interactions. However, further experimental validation is necessary to confirm the association of these 30 putative ciliary proteins with primary cilia and to elucidate their precise roles and locations within the ciliary context.

A

| | Protein Description |
|---|---|
| PPIB | Peptidyl-prolyl cis-trans isomerase B |
| ALDH1A3 | Retinaldehyde dehydrogenase 3 |
| CAVIN1 | Caveolae-associated protein 1 |
| SF3A3 | Splicing factor 3A subunit 3 |
| TRIM25 | E3 ubiquitin/ISG15 ligase TRIM25 |
| AP2A2 | AP-2 complex subunit alpha-2 |
| SRP72 | Signal recognition particle subunit SRP72 |
| CTNND1 | Catenin delta-1 |
| MARS1 | Methionine--tRNA ligase, cytoplasmic |
| HNRNPDL | Heterogeneous nuclear ribonucleoprotein D-like |
| PNPLA6 | Patatin-like phospholipase domain-containing protein 6 |
| CPNE3 | Copine-3 |
| EPHA2 | Ephrin type-A receptor 2 |
| SUPT16H | FACT complex subunit SPT16 |
| RPS7 | Small ribosomal subunit protein eS7 |

| Gene Name | Protein Description |
|---|---|
| CD2AP | CD2-associated protein |
| NUP98 | Nuclear pore complex protein Nup98-Nup96 |
| AP3B1 | AP-3 complex subunit beta-1 |
| GOLGA4 | Golgin subfamily A member 4 |
| CNOT1 | CCR4-NOT transcription complex subunit 1 |
| COPB1 | Coatomer subunit beta |
| NPM1 | Nucleophosmin |
| SERPINH1 | Serpin H1 |
| UACA | Uveal autoantigen with coiled-coil domains and ankyrin repeats |
| TKT | Transketolase |
| AARS1 | Alanine--tRNA ligase, cytoplasmic |
| FLOT2 | Flotillin-2 |
| TJP1 | Tight junction protein ZO-1 |
| NXF1 | Nuclear RNA export factor 1 |
| ARPC1B | Actin-related protein 2/3 complex subunit 1B |

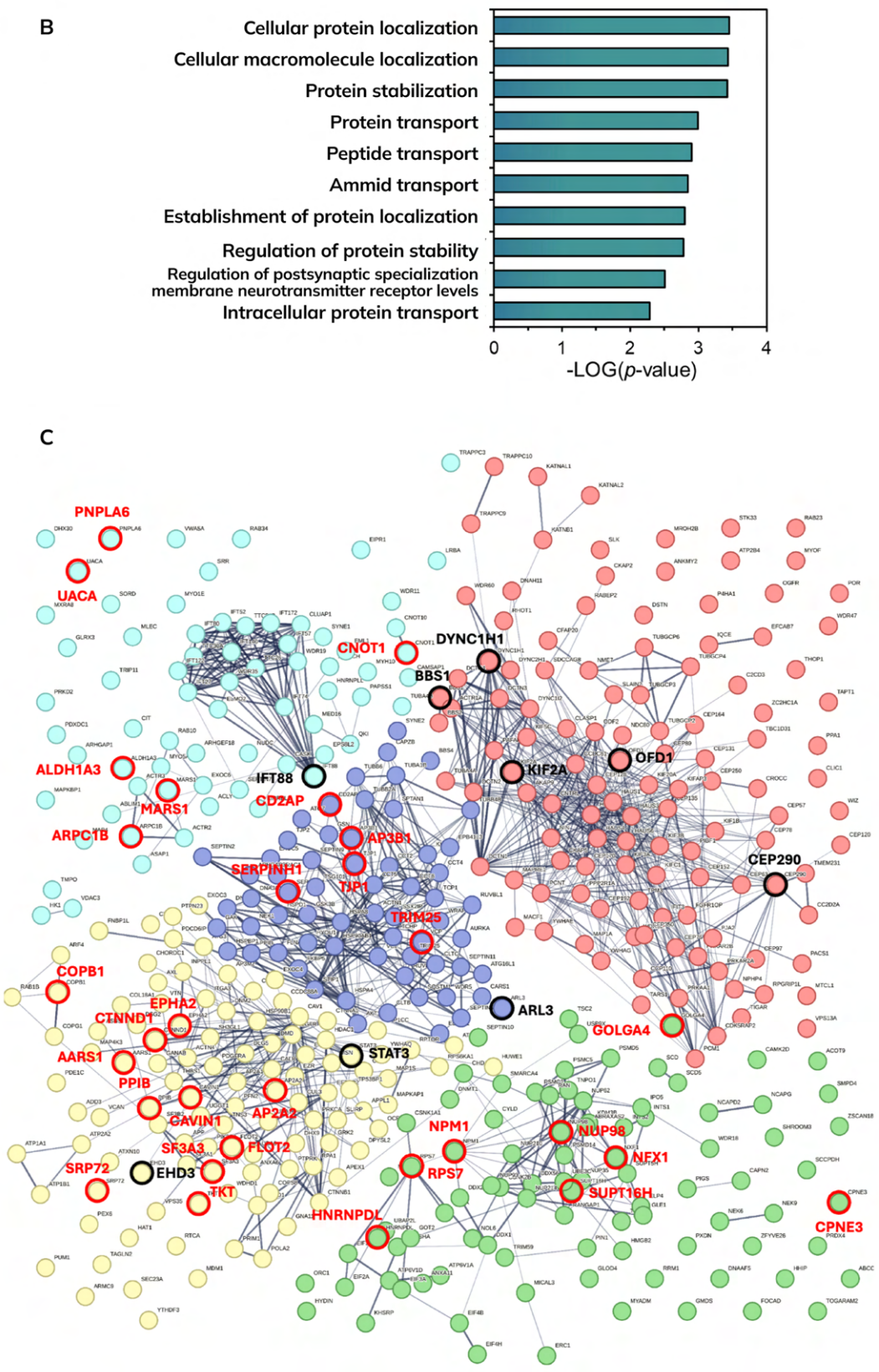


Fig. 5. (A) The list of the top 30 non-ciliary proteins (putative ciliary proteins) enriched by Microscoop™. (B) The top 30 putative ciliary proteins (A) were subjected to Gene ontology to reveal cilia related biological process. (C) The 30 putative ciliary protein and 427 enriched ciliary proteins were subjected to STRING to reveal protein-protein interaction networks, where the 30 putative ciliary proteins are indicated in red and well-known ciliary proteins are indicated in black.

# Conclusion

In this white paper, we present a comprehensive exploration of primary cilia, aiming to deepen our understanding of their composition and biological roles. Our research initiated with the precise targeting and labeling of primary cilia utilizing the Microscoop™ technology, renowned for its accuracy and specificity in photo-biotinylation within primary cilia. This enabled the provision of a comprehensive list of protein candidates associated with primary cilia.

Our findings demonstrate that the Microscoop™ technology effectively enables spatially specific photolabeling of primary cilia, facilitating the identification of both known and novel ciliary proteins and thus enhancing our understanding of this essential cellular component. The total ciliary proteins identified amounted to 608, with significant enrichment of 427 ciliary proteins further analyzed for pathway involvement, revealing key ciliary pathways. The identification of putative ciliary proteins and their interactions with known ciliary proteins opens new avenues for ciliary research, emphasizing the need for further validation studies.

To propel cilia research forward, access to reliable and comprehensive proteomics databases is essential. The currently available open-source cilia databases are fragmented and exhibit inconsistencies, marked by variations in data quality and differences across platforms. This situation, combined with the complexity and small size of primary cilia, presents significant challenges to conducting effective research in this field. In an effort to address these issues, we have collected data from several cilia databases, including Gene Ontology[5], UniProt[6], and CiliaCarta[7], into the SYNCELL database. The ciliary proteome from SYNCELL offers a comprehensive and consistent dataset of ciliary proteins, designed to address the current gaps in research. We aim to empower researchers with the necessary tools for advancing our understanding of ciliary functions and mechanisms.

# References


1. Satir, P. & Christensen, S.T. Overview of structure and function of mammalian cilia. *Annu Rev Physiol* **69**, 377-400 (2007).
2. Brown, J.M. & Witman, G.B. Cilia and Diseases. *Bioscience* **64**, 1126-1137 (2014).
3. Tobin, J.L. & Beales, P.L. Bardet-Biedl syndrome: beyond the cilium. *Pediatr Nephrol* **22**, 926-936 (2007).
4. Cantagrel, V. et al. Mutations in the cilia gene ARL13B lead to the classical form of Joubert syndrome. *Am J Hum Genet* **83**, 170-179 (2008).
5. Ashburner, M. et al. Gene ontology: tool for the unification of biology. The Gene Ontology Consortium. *Nat Genet* **25**, 25-29 (2000).
6. UniProt, C. UniProt: the Universal Protein Knowledgebase in 2023. *Nucleic Acids Res* **51**, D523-D531 (2023).
7. van Dam, T.J.P. et al. CiliaCarta: An integrated and validated compendium of ciliary genes. *PLoS One* **14**, e0216705 (2019).


## For more information, please visit syncell.com


**SYNCELL Inc.**

200 Dexter Ave, Watertown, MA 02472, USA

Info@syncell.com